International Journal of Modern Physics E
Vol. 25, No. 12 (2016) 1650103 (22 pages)

DOI: 10.1142/S0218301316501032

Quest for magicity in hypernuclei

M. Ikram* and Asloob A. Rather†

Department of Physics,
Aligarh Muslim University,
Aligarh-202002, India
**ikram@iopb.res.in*
†*asloobahmad.rs@amu.ac.in*

Bharat Kumar‡, S. K. Biswal§
and S. K. Patra¶

Institute of Physics,
Bhubaneswar-751 005, India
‡*bharat@iopb.res.in*
§*sbiswal@iopb.res.in*
¶*patra@iopb.res.in*

Received 17 July 2016
Revised 27 October 2016
Accepted 11 November 2016
Published 9 December 2016

In the present study, we search the Λ magic number in hypernuclei within the framework of relativistic mean field (RMF) theory with inclusion of hyperon–nucleon and hyperon–hyperon potentials. Based on one- and two-lambda separation energy and two-lambda shell gaps, 2, 8, 14, 18, 20, 28, 34, 40, 50, 58, 68, 70 and 82 are suggested to be the Λ magic numbers within the present approach. The relative weak strength of Λ spin–orbit interaction is responsible for emerging the new lambda shell closures other than the model scheme. The predicted hypernuclear magicity quite resembles with nuclear magicity. In addition, the stability of hypernuclei is also examined by calculating the binding energy per particle, where Ni hypernucleus is found to be most tightly bound triply magic system in considered hypernuclei. Further, nucleon and lambda density distributions are analyzed and it is found that introduced Λ's have significant impact on total density and reduce the central depletion of the core nucleus. Nucleon and lambda spin–orbit interaction potentials are also investigated for predicted triply magic hypernuclei and the addition of Λ's affect both the potentials to a large extent. The single-particle energy levels are analyzed to explain the shell gaps for triply magic multi-Λ hypernuclei.

Keywords: Binding energy; separation energy; single-particle energy; hypernuclei; relativistic mean field theory.

1. Introduction

The study of hypernuclei has been attracting great interest of nuclear physics community in providing the information from nucleon–nucleon (NN) interaction to hyperon–nucleon (YN) and hyperon–hyperon (YY) interactions. Due to the injection of hyperons, a new dimension is added in normal nuclear system and hyperons serve as a potential probe for exploring many nuclear properties in the domain of strangeness.[1–3] However, YN interaction is relatively weaker than NN but it is imperative as well as important to describe the nuclear many-body system with strangeness. Various theoretical approaches such as Skyrme Hartree Fock (SHF),[4–12] relativistic mean field (RMF),[13–18] cluster, variational, diffusion Monte Carlo,[19–29] and G-matrix[30–32] have been employed by scientific community to estimate the strength of YN as well YY interactions. Further, these models have established themselves as very effective in testing the existence of bound hypernuclei and the stability of nucleonic core against hyperon(s) addition or the occurrence of exotic strange matter which facilitates the path toward multi-strange systems.

Magic numbers in nuclear physics are certain neutron and proton numbers in atomic nuclei, in which higher stability in the ground state is observed than in the neighboring nuclides and are most abundant in nature. The various experimental signatures that show discontinuity at magic numbers are the energy required for the separation of one and two nucleons, the energies of alpha and beta transitions, pairing energy and the excitation of low-lying vibrations.[33–35] The separation energy is sensitive to the collective or single particle interplay and provides sufficient information about the nuclear structure effects. The discovery of magic numbers paved the way to great progress in understanding of nuclear structure with some special features and these numbers became the cornerstones in developing the theoretical segment in nuclear physics.

It is worthy to mention that the several signatures are seen for the evolution of the magic gaps along the nuclear chart including superheavy region.[36–38] The quest for proton or neutron magic numbers in the elusive mass region of superheavy nuclei is of utmost importance as the mere existence of superheavy nuclei is the result of the interplay between the attractive nuclear force (shell effects) and the large disruptive coulomb repulsion between the protons that favors the fission.[39,40] It is well established that 2, 8, 20, 28, 50, 82 and 126 are the nucleonic magic numbers. In addition to this, $Z = 120$ and $N = 172$, 184 are predicted to be next magic numbers by various theoretical models in superheavy mass region.[41–45] These predictions have been made on the basis of separation energy, shell gaps, pairing energy and shell correction energy, etc. It may therefore be relevant to extend the line of thought to the hypernuclear chart. It is well known that the spin–orbit interaction in Λ channel is weaker than nucleonic sector and thus the Λ magic numbers are expected to be close to the harmonic oscillator ones: 2, 8, 20, 40 and 70. In this paper, our main motive is to make an extensive investigation to

search the Λ magic number in hypernuclei within the RMF approach and obtain the stability of triply magic system with doubly magic core.

The magic numbers in nuclei are characterized by a large shell gap in single-particle energy levels. This means that the nucleon in the lower level has a comparatively large value of energy than that on higher level giving rise to more stability. The extra stability corresponding to certain number can be estimated from the sudden fall in the separation energy. The Λ separation energy is considered to be one of the key quantities to reveal the nuclear response to the addition of lambda hyperon. Therefore, in the present work, we obtain the binding energy per particle and one-lambda as well as two-lambda separation energies for considered multi-hypernuclei. Moreover, two-lambda shell gap is also calculated to make a clear prediction of magic numbers in hypernuclear regime. To mark the Λ shell gaps, single-particle energy levels are analyzed that may correspond to Λ magic number. In addition, to analyze the structural distribution as well as impact of Λ hyperon on bubble structure for considered nuclei, total (nucleon plus Λ) density is reported. Nucleon and lambda mean field and spin–orbit interaction potentials are also observed. On the basis of binding energy per particle, the stability of triply magic hypernuclei is reported.

RMF theory has been quite successful for studying the infinite nuclear systems and finite nuclei including the superheavy mass region.[41–52] It is quite successful to study the equation of state for infinite nuclear matter as well as pure neutron matter, where the existence of strange baryons is expected.[53,54] In this context, addition of strangeness degree of freedom to RMF formalism is obvious for the suitable extension of the model and such type of attempts have already been made.[14,54–64] RMF explains not only the structural properties of singly strange hypernuclei, but also provides the details study of multi-strange systems containing several Λ's, Σ's or Ξ's. Moreover, RMF explains spin–orbit interaction very nicely in normal nuclei as well as in hypernuclei. The contribution of spin-orbit interaction plays a very crucial role in the emergence of magic number in nucleonic sector and the same is expected in strangeness sector.

The paper is organized as follows: A brief introduction on hypernuclei and magic number is given in Sec. 1. Section 2 gives a brief description of RMF formalism for hypernuclei with inclusion of Λ*N* and ΛΛ interactions. The results are presented and discussed in Sec. 3. The paper is summarized in Sec. 4.

2. Formalism

RMF theory has been applied successfully to study the structural properties of normal nuclei as well as hypernuclei.[14,55–57,59,60,63,64] The suitable extension to hypernuclei is made by including the lambda–baryon interaction Lagrangian with effective ΛN potential. The total Lagrangian density for single-Λ hypernuclei is reported in Refs. 14, 55–57, 59, 60, 63 and 64. For studying the multi-Λ hypernuclei in quantitative manner, additional strange scalar (σ^*) and vector (ϕ) mesons

have been included which simulate the ΛΛ interaction.[54,58,61,62] Now, the total Lagrangian density can be written as

$$\mathscr{L} = \mathscr{L}_N + \mathscr{L}_\Lambda + \mathscr{L}_{\Lambda\Lambda}, \tag{1}$$

$$\begin{aligned}
\mathscr{L}_N &= \bar{\psi}_i\{i\gamma^\mu\partial_\mu - M\}\psi_i + \frac{1}{2}(\partial^\mu\sigma\partial_\mu\sigma - m_\sigma^2\sigma^2) - \frac{1}{3}g_2\sigma^3 \\
&\quad - \frac{1}{4}g_3\sigma^4 - g_s\bar{\psi}_i\psi_i\sigma - \frac{1}{4}\Omega^{\mu\nu}\Omega_{\mu\nu} + \frac{1}{2}m_\omega^2\omega^\mu\omega_\mu \\
&\quad - g_\omega\bar{\psi}_i\gamma^\mu\psi_i\omega_\mu - \frac{1}{4}B^{\mu\nu}B_{\mu\nu} + \frac{1}{2}m_\rho^2\boldsymbol{\rho}^\mu\boldsymbol{\rho}_\mu - \frac{1}{4}F^{\mu\nu}F_{\mu\nu} \\
&\quad - g_\rho\bar{\psi}_i\gamma^\mu\boldsymbol{\tau}\psi_i\boldsymbol{\rho}^\mu - e\bar{\psi}_i\gamma^\mu\frac{(1-\tau_{3i})}{2}\psi_i A_\mu, \\
\mathscr{L}_\Lambda &= \bar{\psi}_\Lambda\{i\gamma^\mu\partial_\mu - m_\Lambda\}\psi_\Lambda - g_{\sigma\Lambda}\bar{\psi}_\Lambda\psi_\Lambda\sigma - g_{\omega\Lambda}\bar{\psi}_\Lambda\gamma^\mu\psi_\Lambda\omega_\mu, \\
\mathscr{L}_{\Lambda\Lambda} &= \frac{1}{2}(\partial^\mu\sigma^*\partial_\mu\sigma^* - m_{\sigma^*}^2\sigma^{*2}) - \frac{1}{4}S^{\mu\nu}S_{\mu\nu} + \frac{1}{2}m_\phi^2\phi^\mu\phi_\mu \\
&\quad - g_{\sigma^*\Lambda}\bar{\psi}_\Lambda\psi_\Lambda\sigma^* - g_{\phi\Lambda}\bar{\psi}_\Lambda\gamma^\mu\psi_\Lambda\phi_\mu,
\end{aligned} \tag{2}$$

where ψ and ψ_Λ denote the Dirac spinors for nucleon and Λ-hyperon, whose masses are M and m_Λ, respectively. Because of zero isospin, the Λ-hyperon does not couple to ρ- mesons. The quantities m_σ, m_ω, m_ρ, m_{σ^*}, m_ϕ are the masses of σ, ω, ρ, σ^*, ϕ mesons and g_s, g_ω, g_ρ, $g_{\sigma\Lambda}$, $g_{\omega\Lambda}$, $g_{\sigma^*\Lambda}$, $g_{\phi\Lambda}$ are their coupling constants, respectively. The nonlinear self-interaction coupling of σ mesons is denoted by g_2 and g_3. The total energy of the system is given by $E_{\text{total}} = E_{\text{part}}(N,\Lambda) + E_\sigma + E_\omega + E_\rho + E_{\sigma^*} + E_\phi + E_c + E_{\text{pair}} + E_{\text{c.m.}}$, where $E_{\text{part}}(N,\Lambda)$ is the sum of the single-particle energies of the nucleons (N) and hyperon (Λ). The energy parts E_σ, E_ω, E_ρ, E_{σ^*}, E_ϕ, E_c, E_{pair} and E_{cm} are the contributions of meson fields, Coulomb field, pairing energy and the center-of-mass energy, respectively. In the present work, for meson–baryon coupling constant, NL3* parameter set is used throughout the calculations.[65] To find the numerical values of used Λ-meson coupling constants, we adopt the nucleon coupling to hyperon couplings ratio defined as; $R_\sigma = g_{\sigma\Lambda}/g_\sigma$, $R_\omega = g_{\omega\Lambda}/g_\omega$, $R_{\sigma^*} = g_{\sigma^*\Lambda}/g_\sigma$ and $R_\phi = g_{\phi\Lambda}/g_\omega$. The relative coupling values are used as $R_\omega = 2/3$, $R_\sigma = 0.6104$, $R_\phi = -\sqrt{2}/3$ and $R_{\sigma^*} = 0.69$.[61,66,67] The coupling constants of hyperons to vector mesons have to be compatible with the maximum neutron star masses and are fitted to the Λ binding energy in nuclear matter.[68] In the present calculations, we use the constant gap BCS approximation to include the pairing interaction and the center-of-mass correction is included by $E_{\text{cm}} = -(3/4)41A^{-1/3}$.

3. Results and Discussions

Before taking a detour on searching the Λ magic behavior in multi-Λ hypernuclei, first we shall see the effects of introduced Λ hyperons on normal nuclear core i.e.,

how the binding energy and radii of normal nuclear system is affected by addition of Λ's? To analyze this, we consider a list of normal nuclei covering a range from light to superheavy mass region, i.e. ^{16}O to ^{378}120. Binding energy per particle (BE/A), lambda binding energy (B_Λ) for s- and p- states and radii for considered core nuclei and corresponding hypernuclei are tabulated in Table 1. The calculated B_Λ is compared with available experimental data wherever available and we found a close agreement between them. For example, the Λ binding energy for s- and p-states in our RMF calculation is found to be -12.09 MeV and -2.66 MeV for $^{16}_{\Lambda}$O, whereas the experimental values for corresponding states are -12.5 ± 0.35 MeV and 2.5 ± 0.5 MeV, respectively. Also, the calculated BE/A employing RMF with NL3* and NL3 are compared with each other and with FSU,[70] SHF[71] where we noticed a close agreement among them. This means the used parameter set (NL3*) is quite efficient to reproduce the experimental binding energy and is consistent with other parameter sets as mentioned above. Further, we can exploit it to make more calculations related to magicity in hypernuclei. Since we are dealing with closed shell hypernuclei, our RMF calculations are restricted to spherical symmetric case.

The addition of Λ hyperon to normal nuclei enhances the binding and shrinks the core of the system. This happens because of glue-like role of Λ hyperon that resides on the s-state for most of the time. These observations are shown in Table 1, where the binding energy of hypernuclei becomes larger than their normal counter parts and a reduction in total radius (r_{total}) is observed. In other words, the Λ particle makes the core compact with increasing binding. For example, the total radius of ^{16}O and ^{209}Pb is 2.541 fm and 5.624 fm, which reduces to 2.536 fm and 5.616 fm by addition of a single Λ into the core of O and Pb, respectively. Moreover, for the sake of comparison with experimental data, binding energy and radii of the hypernuclei produced by replacing the neutrons means having a constant baryon number are also framed in Table 1 and the shrinkage effect is also noticed there. These results show the impact of injected Λ hyperons on binding as well as size of the considered doubly magic nuclear cores.

3.1. *Stability of hypernuclei*

Binding energy provides the detailed information of various elements corresponding to their stability. Binding energy per particle increases upto the element iron whose atomic number is 26 and mass number's 57. The information provided by the binding energy per particle curve is that iron and its neighboring elements (Ni) are most stable, i.e., they neither undergo fission or fusion. Thus, the significance of the binding energy per particle curve lies in the fact that it is an indicator of nuclear stability and thus helps in classifying the elements which undergo fission, fusion and radioactive disintegration. We noticed a similar pattern of binding energy per particle in hypernuclear regime also. The triply magic system is produced by addition of Λ magic number into the core of doubly shell closure such as ^{16}O, ^{48}Ca, ^{58}Ni, ^{90}Zr, ^{124}Sn, ^{132}Sn, ^{208}Pb, ^{292}120, ^{304}120, ^{378}120. Binding energy

Table 1. The calculated binding energy per particle for single-Λ hypernuclei are listed here. The Λ binding energy for s- and p-state of considered hypernuclei are also mentioned and compared with available experimental values,[69] are given in parentheses. Calculated binding energy per particle employing NL3* and NL3 are compared with each other and also with RMF (FSU)[70] and SHF,[71] wherever available. The radii are also displayed. Binding energy are given in unit of MeV and radii are in Fermi.

Nuclei/Hypernuclei	BE/A (NL3*)	BE/A (NL3)	BE/A (FSU)	BE/A (SHF)	B^s_Λ	B^p_Λ	$r_{\rm ch}$	$r_{\rm total}$	r_p	r_n	r_Λ
^{16}O	7.89	7.94					2.674	2.541	2.555	2.527	
$^{16}_{\Lambda}$O	7.77	7.84			-12.09 (12.5 ± 0.35)	-2.66 (2.5 ± 0.5)	2.673	2.487	2.550	2.428	2.388
$^{17}_{\Lambda}$O	8.12	8.19	8.25		-11.98	-3.07	2.673	2.536	2.554	2.526	2.468
^{40}Ca	8.54	8.54					3.446	3.331	3.355	3.307	
$^{40}_{\Lambda}$Ca	8.60	8.62			-17.51 (18.7 ± 1.1)	-9.32 (11.0 ± 0.6)	3.439	3.292	3.346	3.262	2.693
$^{41}_{\Lambda}$Ca	8.75	8.77	8.78		-17.39	-9.46	3.444	3.315	3.352	3.304	2.737
^{48}Ca	8.63	8.65					3.444	3.496	3.359	3.591	
$^{48}_{\Lambda}$Ca	8.86	8.89			-18.75	-10.95	3.439	3.459	3.353	3.558	2.785
$^{49}_{\Lambda}$Ca	8.84	8.87	8.82	8.75	-18.94	-11.16	3.440	3.479	3.355	3.586	2.791
^{56}Ni	8.61	8.63					3.696	3.586	3.610	3.561	
$^{56}_{\Lambda}$Ni	8.71	8.73			-20.48	-12.67	3.695	3.560	3.609	3.533	2.816
$^{57}_{\Lambda}$Ni	8.82	9.18			-20.72	-12.89	3.689	3.567	3.603	3.555	2.817
^{90}Zr	8.70	8.70					4.249	4.245	4.179	4.297	
$^{90}_{\Lambda}$Zr	8.80	8.59			-21.28	-15.25	4.246	4.221	4.175	4.277	3.215
$^{91}_{\Lambda}$Zr	8.84	8.62		8.73	-21.37	-15.36	4.247	4.233	4.177	4.295	3.222

Table 1. (*Continued*)

Nuclei/Hypernuclei	BE/A (NL3*)	BE/A (NL3)	BE/A (FSU)	BE/A (SHF)	B^s_Λ	B^p_Λ	$r_{\rm ch}$	$r_{\rm total}$	r_p	r_n	r_Λ
^{124}Sn	8.45	8.46					4.642	4.753	4.580	4.866	
$^{124}_{\Lambda}$Sn	8.55	8.58		8.55	-22.24	-17.10	4.633	4.729	4.571	4.849	3.493
$^{125}_{\Lambda}$Sn	8.57	8.57			-22.28	-17.17	4.638	4.742	4.577	4.864	3.503
^{132}Sn	8.35	8.37					4.689	4.854	4.631	4.985	
$^{132}_{\Lambda}$Sn	8.47	8.50			-22.56	-17.65	4.680	4.830	4.620	4.969	3.570
$^{133}_{\Lambda}$Sn	8.46	8.48			-22.60	-17.71	4.686	4.843	4.627	4.983	3.579
^{208}Pb	7.88	7.88					5.499	5.624	5.448	5.736	
$^{208}_{\Lambda}$Pb	7.78	7.97			-23.56 (26.3 ± 08)	-19.74 (21.3 ± 0.7)	5.492	5.604	5.441	5.719	4.067
$^{209}_{\Lambda}$Pb	7.96	8.07	7.96	7.89	-23.54	-19.76	5.496	5.616	5.445	5.734	4.076
$^{292}120$	7.06	7.06					6.271	6.322	6.225	6.389	
$^{292}_{\Lambda}120$	7.12	7.12			-23.73	-20.94	6.262	6.306	6.216	6.376	3.316
$^{293}_{\Lambda}120$	7.21	7.04			-23.59	-20.86	6.268	6.316	6.223	6.387	3.320
$^{304}120$	7.04	7.04					6.302	6.417	6.258	6.519	
$^{304}_{\Lambda}120$	7.19	7.11			-23.89	-21.03	6.298	6.403	6.253	6.507	3.272
$^{305}_{\Lambda}120$	7.18	7.10			-23.79	-20.96	6.300	6.411	6.255	6.518	3.301
$^{378}120$	6.31	6.34					6.714	7.144	6.678	7.350	
$^{378}_{\Lambda}120$	6.11	6.46			-23.09	-20.81	6.896	7.344	6.863	7.543	3.642
$^{379}_{\Lambda}120$	6.09	6.45			-23.43	-21.04	6.712	7.138	6.676	7.350	3.549

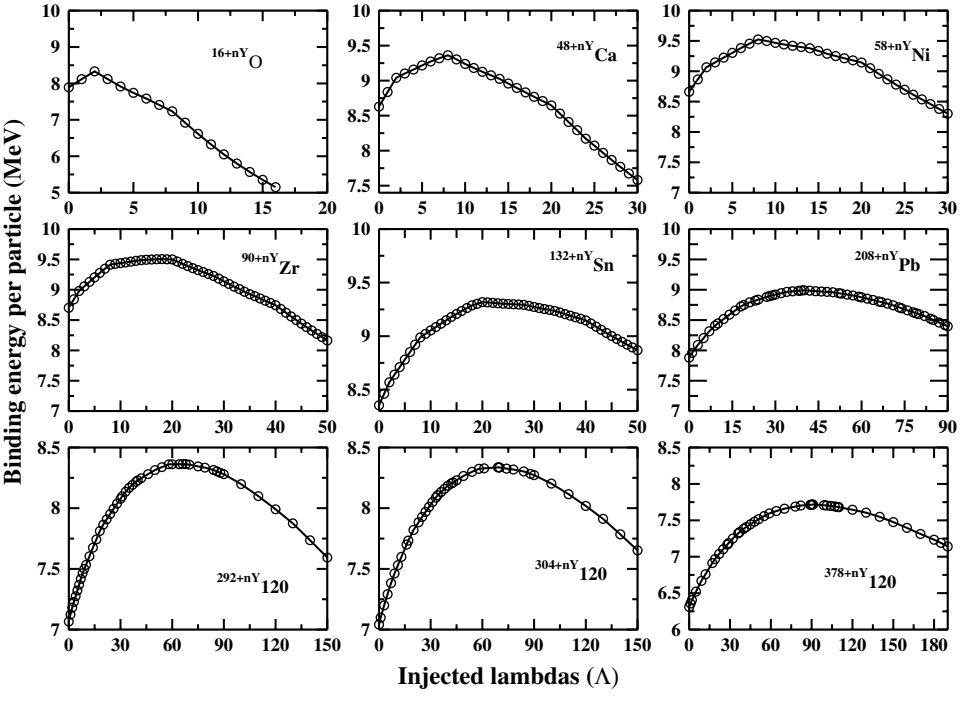

Fig. 1. Binding energy per particle for light to superheavy mass multi-Λ hypernuclei.

per particle of considered hypernuclear systems confirms that nickel with 8 Λ's ($^{56+8\Lambda}$Ni) is the most tightly bound hypernucleus (BE/A = 9.5 MeV) as shown in Fig. 1. These results are in remarkable agreement with earlier predictions.[61,62]

3.2. *Binding energy and separation energy*

To analyze the magic behavior of lambda in multi-Λ hypernuclei, we choose the nuclear core of doubly shell closure including predicted shell closure nuclei of superheavy mass region and then add the Λ hyperons to the closed shell nuclei to see the effects of hyperon addition. Here, we look for the binding energy per particle with respect to added hyperons for considered hypernuclei as given in Fig. 1. The peak value of the graph corresponds to maximum stability for a particular hypernuclear system. It also explains that the injection of few Λ hyperons enhance the binding of the light mass hypernuclei and the further addition reduces the binding energy of the light and superheavy mass multi-hypernuclei. However, for the heavy mass region, the BE/A increases with addition of large number of hyperons and forms the a most bound system, but further addition decreases the binding energy gradually. This means certain number of added Λ's to a particular nuclear core form the most stable system. For example, the injection of 2 Λ's provides the maximum stability to ^{16}O. Proceeding along similar lines, a maximum binding is observed for ^{48}Ca with

$\Lambda = 8$ and this number goes to 90 for the superheavy core. In this way, we extract certain numbers of added Λ's, that is, 2, 8, 18, 20, 40, 70, 90 which provide maximum stability for the considered systems (i.e., $^{16+2\Lambda}$O, $^{48+8\Lambda}$Ca, $^{58+8\Lambda}$Ni, $^{90+18\Lambda}$Zr, $^{124+20\Lambda}$Sn, $^{132+20\Lambda}$Sn, $^{208+40\Lambda}$Pb, $^{292+68\Lambda}120$, $^{304+70\Lambda}120$, $^{378+90\Lambda}120$) and these numbers may correspond to Λ magic number in multi-Λ hypernuclei. It is the not only the criterion, but there also exist several strong signatures of marking the magic number, such as separation energy, shell gaps, pairing energy etc. Therefore, to analyze the actual behavior of magicity, we analyze such relevant parameters. In this regard, we estimate one- and two-lambda separation energy S_Λ and $S_{2\Lambda}$, which are known to provide the first insight of shell closure. In analogy to nucleonic sector, the magic number in multi-hypernuclei may be characterized by the large lambda shell gaps in single-particle energy levels. The extra stability provided by certain number of introduced Λ's can also be noticed from sudden fall in Λ separation energy. Therefore, for searching the magicity in multi-Λ hypernuclei, one- and two-lambda separation energy is estimated using the following expressions:

$$S_\Lambda(N, Z, \Lambda) = \mathrm{BE}(N, Z, \Lambda) - \mathrm{BE}(N, Z, \Lambda - 1)$$

and

$$S_{2\Lambda}(N, Z, \Lambda) = \mathrm{BE}(N, Z, \Lambda) - \mathrm{BE}(N, Z, \Lambda - 2).$$

These quantities are plotted in Figs. 2–5. For a lambda chain, the S_Λ and $S_{2\Lambda}$ become larger with increasing number of lambda Λ. For a fixed Z, N, S_Λ and $S_{2\Lambda}$ decrease gradually with lambda number. A sudden decrease of S_Λ and $S_{2\Lambda}$ just after

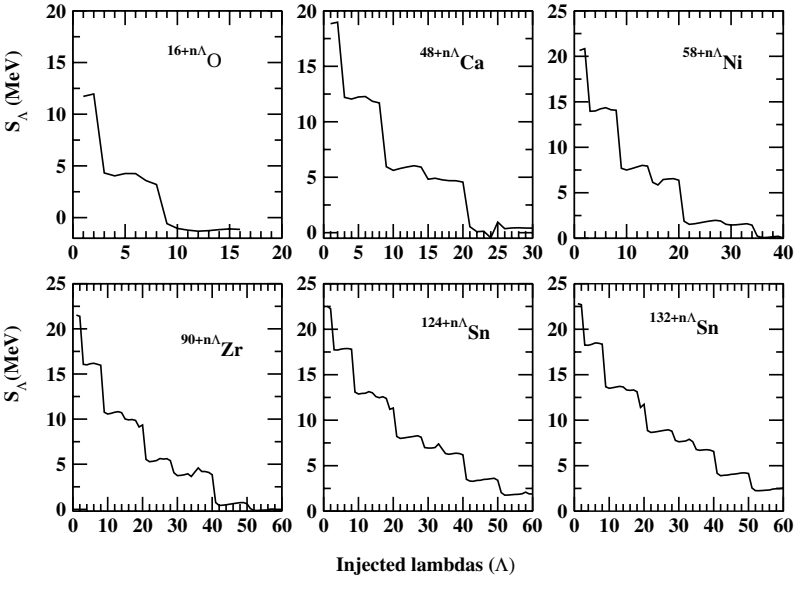

Fig. 2. One lambda separation energy for medium mass multi-Λ hypernuclei.

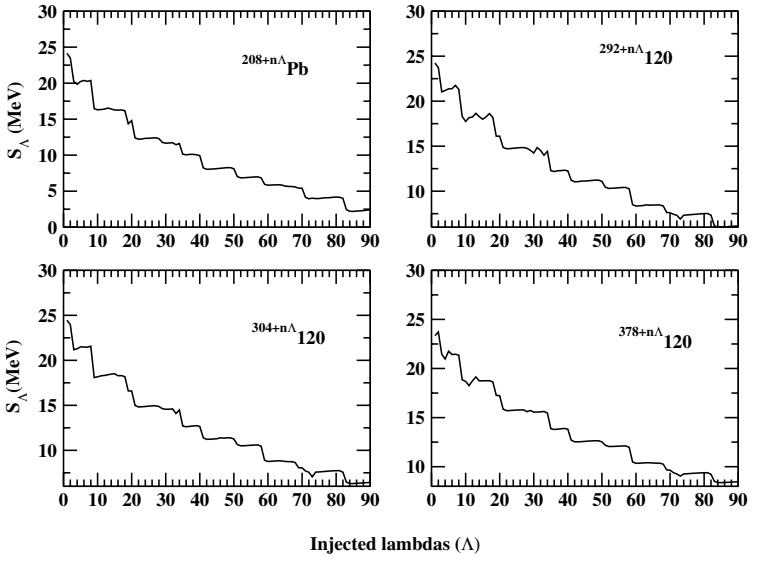

Fig. 3. Same as Fig. 2 but for heavy to superheavy mass multi-Λ hypernuclei.

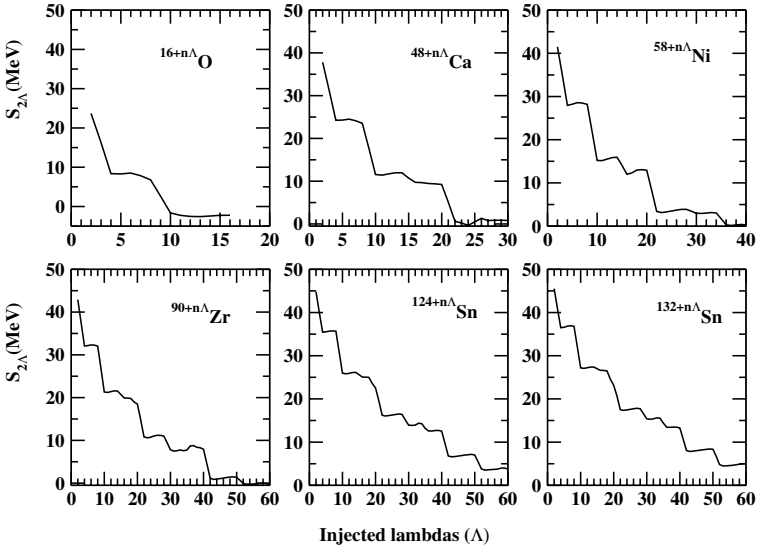

Fig. 4. Two lambda separation energy for medium mass multi-Λ hypernuclei.

the magic number in lambda chain-like as neutron chain indicates the occurrence of Λ shell closure. The sudden fall of S_Λ at $\Lambda = 2, 8, 14, 18, 20, 28, 34, 40, 50, 58, 68, 70$ and 82 can clearly be seen in considered hypernuclear candidates revealing a signature of magic character. Moreover, $\Lambda = 14$ and 28 are observed only in light mass mulit-Λ hypernuclei, even $\Lambda = 28$ does not show pronounced energy separation.

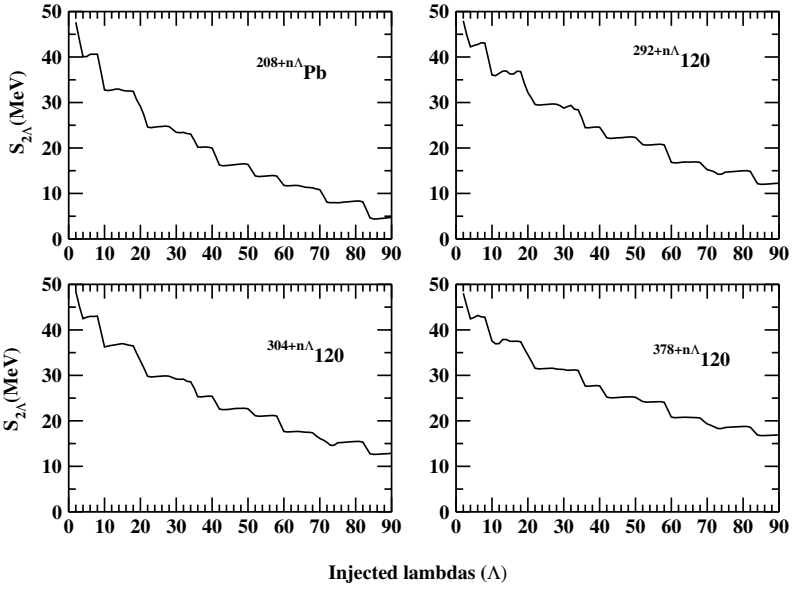

Fig. 5. Same as Fig. 4 but for heavy to superheavy mass multi-Λ hypernuclei.

However, a good strength of sudden fall of S_Λ at $\Lambda = 34$ and 58 is clearly observed in heavy and superheavy mass region.

Two-lambda separation energy provides more strong signature to quantify shell closure due to the absence of odd–even effects. Figures 4 and 5 reveal that sudden fall of $S_{2\Lambda}$ at $\Lambda = 2, 8, 14, 18, 20, 28, 34, 40, 50, 58, 68, 70$ and 82 is observed in considered multi-Λ hypernuclear candidates. These certain numbers correspond to Λ magic number in multi-Λ hypernuclei and form a triply magic system with doubly magic core. This is the central theme of the paper. The significant fall of S_Λ and $S_{2\Lambda}$ at $\Lambda = 14$ appears in Ca and Ni hypernuclei. The lambda number 28 seems to be a very feeble magic number, contrary to nucleonic sector. Another new lambda number 68 supposed to be semi-magic arises due to subshell closure. For the sake of clear presentation of the results, we also analyze for two-lambda shell gaps ($\delta_{2\Lambda}$), which are plotted as a function of added Λ's.

Summarizing the above results, we may say that based on one- and two-lambda separation energies S_Λ and $S_{2\Lambda}$, the signatures of the magicity in RMF appear at 2, 8, 14, 18, 20, 28, 34, 40, 50, 58, 68, 70 and 82. The lambda numbers 28 and 68 appear in light and heavy hypernuclei, respectively, and are supposed to be feeble magic number.

3.3. *Two-lambda shell gap*

The change of the two-lambda separation energies can also be quantified by the second difference of the binding energies, i.e., two-lambda shell gap which is

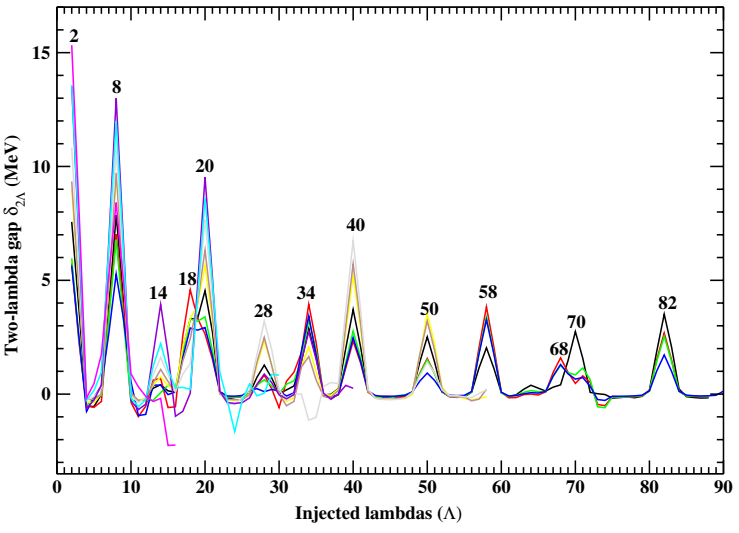

Fig. 6. (Color online) Two lambda shell gap is shown for considered multi-Λ hypernuclei.

expressed by

$$\delta_{2\Lambda}(N,Z,\Lambda) = 2\mathrm{BE}(N,Z,\Lambda) - \mathrm{BE}(N,Z,\Lambda+2) - \mathrm{BE}(N,Z,\Lambda-2)$$
$$= S_{2\Lambda}(N,Z,\Lambda) - S_{2\Lambda}(N,Z,\Lambda+2).$$

A peak of two-lambda shell gaps indicates the drastic change of the two-lambda separation energies, which serves as one of the significant signatures of the magic number. The two-lambda shell gaps, $\delta_{2\Lambda}$, for all considered hypernuclei as a function of added Λ hyperons are shown in Fig. 6. A peak at certain Λ number suggests the existence of lambda shell closure. However, the quality of magic number is represented by sharpness as well as the magnitude of the peak. Figure 6 reveals that the magnitude of the peak is found to be largest at $\Lambda = 2, 8, 20, 40$ indicating the strong shell closures. Further, the peaks appearing at $\Lambda = 14, 18, 28, 34, 50, 58, 70$ and 82 indicate the respective lambda magic number. Moreover, a peak with a very small magnitude also appearing at $\Lambda = 68$ due to closure of subshell $(2d_{3/2})$ reveals Λ semi-magic number. A peak with small magnitude is seen at $\Lambda = 28$ representing a feeble lambda magic number, contrary to the strong nucleonic magic number. A pronounced peak appears at $\Lambda = 34$ and 58 indicating a strong Λ closed shells.

3.4. *Density profile and bubble structure*

A hypernucleus is a composed system of nucleons and hyperons and hence the gross structure of hypernucleus can be described by density distribution of nucleons as well as hyperons. It is well known and has been mentioned earlier in the paper that the addition of a Λ hyperon makes the nuclear core compact with increasing binding as well as density. Therefore, it is interesting to study the effects of large number

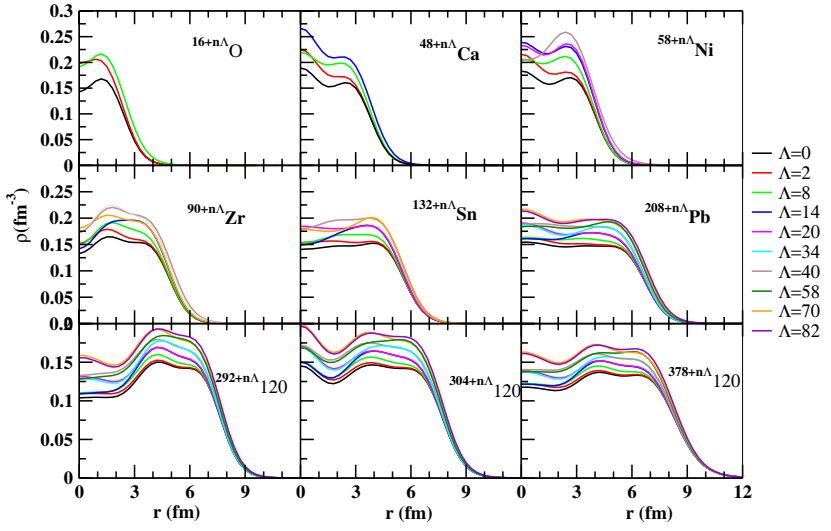

Fig. 7. (Color online) Total (Nucleon plus lambda) density for considered triply magic hypernuclei with $\Lambda = 0, 2, 8, 14, 20, 34, 40, 58, 70$ and 82.

of added Λ hyperons on the nuclear density. Due to the addition of hyperons, the magnitude of total density increases with increasing number of Λ's as shown in Fig. 7. On viewing the density profile, one can examine the most interesting feature of nuclei, i.e., bubble structure, which measures the depletion of central density and has already been observed in light to superheavy mass region.[10,60,72,73] It is to be noticed that several factors, including pairing correlations,[73] tensor force[74,75] and dynamic shape fluctuations[76–78] turn out to have influence on the depletion of central density. The exotic structures like bubble and halo have been recently studied in Λ-hypernuclei.[79]

Owing to weaker $\Lambda\Lambda$ attraction compared to the NN one, the lambda hyperons are more diffused in a nucleus than nucleons and thus generating a hyperon density about 1/3 smaller than the nucleonic density. Thus, it becomes quite important to look for the effect of large number of hyperons on neutron and proton density distributions. Since there is no change of nucleon number, no anomalous effect of introduced Λ's on neutron and proton densities is observed, individually. But the total density of the system is largely affected due to increasing number of Λ's into the core. In the considered multi-hypernuclei, the nucleonic core of some of them shows the depletion of central density for example ^{16}O, ^{90}Zr, $^{292}120$, $^{304}120$ and $^{378}120$ as predicted earlier also.[60,72] It is found that the injected Λ's reduce the depletion of central density. For example, the depletion of central part in ^{16}O is reduced by injection of 2 Λ's and furthermore by the addition of eight Λ's. The Λ particle attracts the nucleons towards the center enhancing the central density and as a result removes the bubble structure partially or fully as reflected in Fig. 7. Therefore, it is one of the important implications of Λ particle to the nuclear system.

Beyond the bubble structure, no anomalous behavior of total density (core +Λ) in triply magic system is reported.

3.5. *Spin–orbit interaction potentials*

The spin–orbit interaction plays a significant role in reproducing the empirical magic numbers. It is a plus point of RMF in which the spin–orbit splitting is built-in naturally and thus describes the nuclear fine structure. The spin–orbit interaction of baryons arises from the difference of the scalar and vector potentials. Thus, by recasting the Dirac equation into the schrödinger equivalent form, we obtain the spin–orbit potential of baryons in the following form:

$$V_{\rm ls} l.s = \frac{1}{2M_{\rm eff}^2}\left[\frac{1}{r}\left(g_\omega \frac{\partial \omega_0}{\partial r} - g_\sigma \frac{\partial \sigma}{\partial r}\right)\right] l.s,$$

where

$$M_{\rm eff} = M - \frac{1}{2}(g_\omega \omega_0 + g_\sigma \sigma).$$

It is not limited only to nuclei or superheavy nuclei but appears in hypernuclei also, however, the strength of interaction is weaker than normal nuclei.[56,80,81] The hyperon-nucleon interaction involves the coupling of scalar ($g_{\sigma\Lambda}$) and vector ($g_{\omega\Lambda}$) mesons with the lambda hyperon. Proceeding along the similar lines, we obtain the lambda spin–orbit potential in the same form as in baryonic case with the coupling constants of sigma and omega mesons with nucleon being replaced by their coupling with lambda hyperon.

$$V_{\rm ls}^{\Lambda} l.s = \frac{1}{2M_{\rm eff}^2}\left[\frac{1}{r}\left(g_{\omega\Lambda} \frac{\partial \omega_0}{\partial r} - g_{\sigma\Lambda} \frac{\partial \sigma}{\partial r}\right)\right] \text{l.s}$$

where

$$M_{\rm eff} = M_\Lambda - \frac{1}{2}(g_{\omega\Lambda} \omega_0 + g_{\sigma\Lambda} \sigma).$$

It is clearly seen from Fig. 8 that the spin–orbit potential for lambda hyperon is weaker than their normal counter parts and our results are consistent with theoretical predictions and experimental measurements.[82–84] Here, nucleon ($V_{\rm so}^N$) and lambda ($V_{\rm so}^\Lambda$) spin–orbit interaction potentials are calculated and plotted for considered triply magic multi-hypernuclei. It is also concluded that the addition of Λ's affects the nucleon as well as Λ spin–orbit potential to a great extent.

3.6. *Single-particle energies*

Any kind of changes in a quantum many-body system, for example, a nucleus can be observed from the single-particle energy level spectrum. To analyze the impact of Λ hyperon on nucleon single-particle energy levels, the filled neutron and proton levels for Ca hypernuclei are plotted as a function of added hyperons as shown in Fig. 9. Figure 9 reveals that the neutron and proton energy levels go deeper with addition

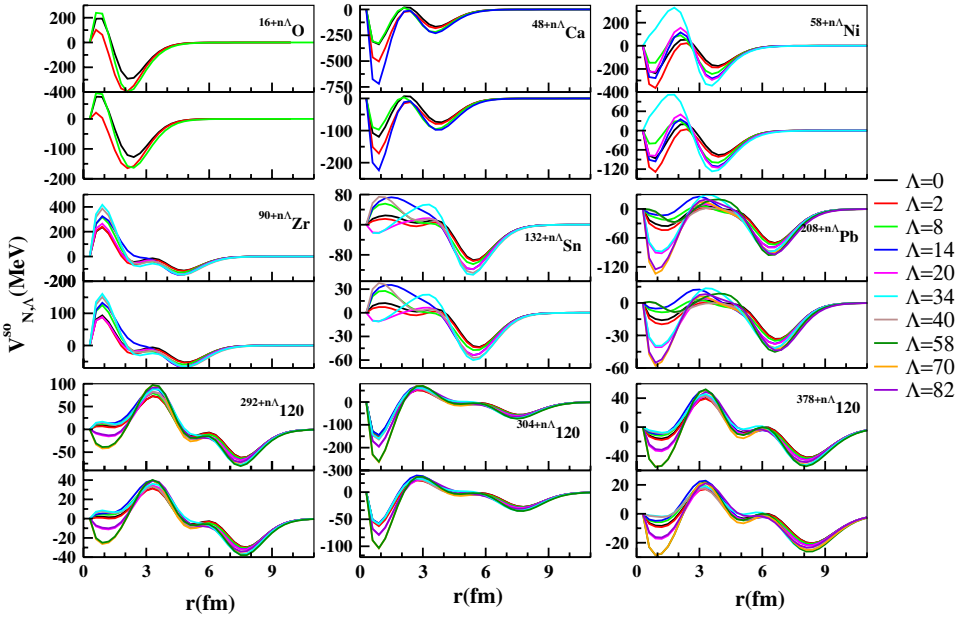

Fig. 8. (Color online) Spin–orbit interaction potentials of nucleon and lambda for considered triply magic hypernuclei with $\Lambda = 0, 2, 8, 14, 20, 34, 40, 58, 70$ and 82. The upper part in each panel represents the nucleonic spin–orbit and the lower one representing the lambda spin–orbit interaction.

of Λ's and as a result they increase the stability of the system. The added hyperons increase the nucleon separation energy and as a result form a more bound system with increasing binding energy than their normal counter parts, which also leads to an extension of drip-line.[29] For example, neutron $s_{1/2}$(n) level has an energy of about -54.037 MeV for the core of Ca hypernucleus, while this amount reaches to -62.499 MeV for $^{48+18\Lambda}$Ca system with 18 Λ's. Also, a same trend is observed for proton levels where, $s_{1/2}$(p) has an energy 51.787 MeV for the core of Ca hypernuclei and this value reaches -60.0477 MeV with addition of 18 Λ's. These results show that the addition of Λ hyperons draws the nuclear system towards more stability with increasing strangeness. Moreover, the same trend of neutron and proton energy levels is observed for other multi-hypernuclei where both the levels would go deeper with increasing number of Λ hyperon to nucleonic core but for the sake of clarity the neutron and proton single-particle energy levels are not plotted here. An inversion of proton levels is seen, where $d_{3/2}$ fills faster than $s_{1/2}$ and this type of filling is also observed in lambda levels. Further, we analyze the lambda single-particle energy levels for $^{48+n\Lambda}$Ca, $^{208+n\Lambda}$Pb and $^{304+n\Lambda}$120 hypernuclei to extract the lambda shell gaps for confirming the Λ magic number. The lambda energy levels as a function of added Λ's are given in Figs. 9–11. The filling of Λ's is same as the nucleons following the shell model scheme with lambda spin–orbit interaction potential. It is observed that the single-particle gap of spin–orbit splitting in lambda levels is smaller than

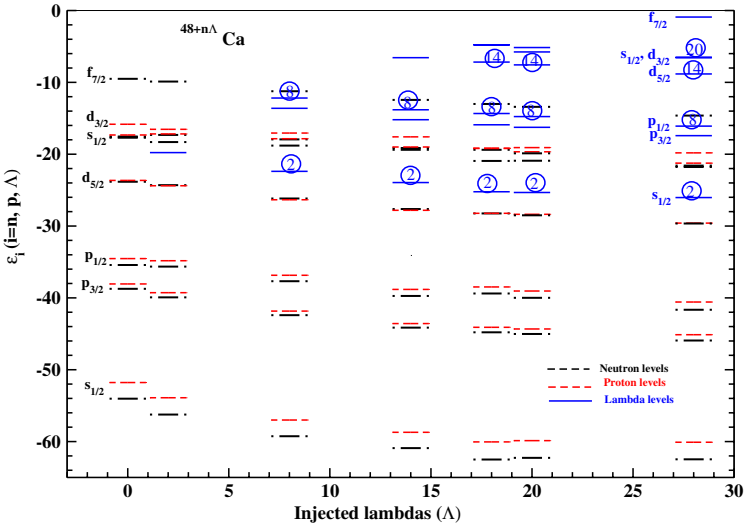

Fig. 9. (Color online) Single-particle energy levels for triply magic Ca multi-hypernuclei for $\Lambda = 2, 8, 14, 18, 20$ and 28.

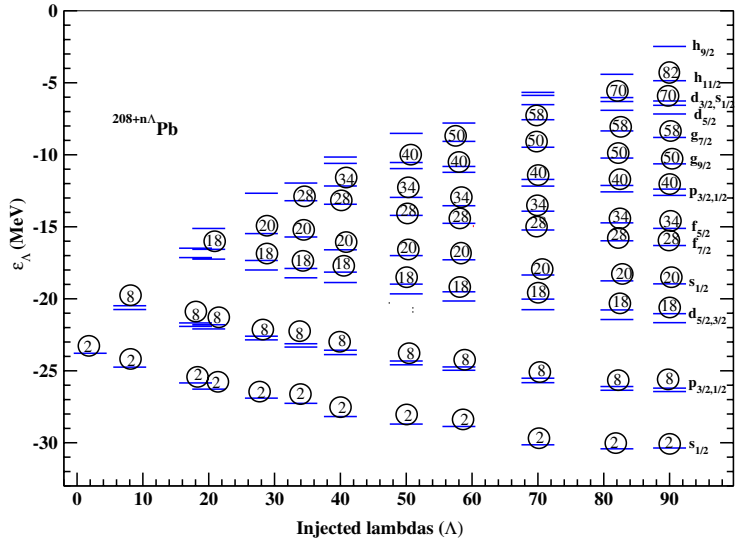

Fig. 10. (Color online) Single-particle energy levels for triply magic Pb multi-hypernuclei for $\Lambda = 2, 8, 18, 20, 28, 34, 40, 50, 58, 70, 82$ and 90.

the nucleons due to relative weaker strength of lambda spin–orbit interaction. By analyzing the lambda single-particle energy levels of Ca hypernuclei, it is found that large energy gap exist in $1d_{5/2}$ to $1d_{3/2}$ or $1d_{5/2}$ to $2s_{1/2}$ and that's why lambda magic number 14 emerges. Further, $2s_{1/2}$ and $1d_{3/2}$ are very much close to each other due to weaker strength of Λ spin–orbit interaction. In case of Pb, the

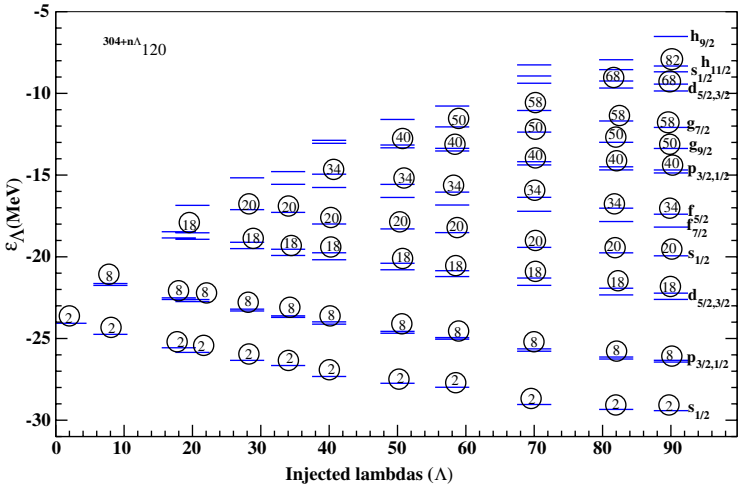

Fig. 11. (Color online) Single-particle energy levels for triply magic $^{304}120$ multi-hypernuclei for $\Lambda = 2, 8, 18, 20, 28, 34, 40, 50, 58, 70, 82$ and 90.

large shell gaps corresponding to $\Lambda = 2, 8, 18, 20, 28, 34, 40, 50, 58, 70$ and 82 appear. However, the single-particle gap for lambda number 28 is not so strong as compared to others suggesting the feeble magic number. The inversion of normal level scheme is noticed and the higher levels fill faster than lower one and hence this type of filling is responsible for the emergence of the new more magic numbers. For example, the filling of $1d_{3/2}$ before $2s_{1/2}$ shows a shell gap at $\Lambda = 18$. Along the similar lines, due to inversion between $\{1f_{5/2}, 2p_{3/2}\}$ and $\{1g_{7/2}, 2d_{5/2}\}$, the Λ closed shells 34 and 58 are observed, respectively. In case of superheavy multi-hypernuclei, large single-particle shell gaps appear for lambda number 2, 8, 18, 20, 34, 40, 50, 58, 70 and 82. It is quite worthy to mention here that pronounced energy gaps are noticed in ^{208}Pb and $^{304}120$ at $\Lambda = 34$, 58 and are being thus suggested to be strong Λ shell closures. The sharp peaks observed in $\delta_{2\Lambda}$ at $\Lambda = 2, 8, 20, 34, 40$ and 58 are clearly reflected from lambda single-particle energies, where a large energy gap exists by filling of these number of lambda hyperons.

3.7. *Magicity*

Various signatures of the evolution of magic shell gaps have been discovered across the nuclear landscape during the past few decades[37,38] such as (i) a large binding energy than neighboring nuclides, (ii) sudden fall at separation energy, (iii) a large shell gap, etc. It becomes therefore quite relevant to extend the prediction of magic numbers to the hypernuclear chart. Looking for the magic behavior first, we emphasize on binding of some selected nuclei whose nucleonic core is doubly magic such as O, Ca, Ni, Zr, Sn, Pb and 120. The injection of certain number of Λ hyperons binds the nuclear core with maximum stability that may correspond to Λ magic number in hypernuclei and might form a triple magic system with doubly

magic core as initially discussed in Ref. 13 and recently in Ref. 79. For example, the addition of $\Lambda = 2$ produces a maximum binding for ^{16}O while the binding energy of ^{48}Ca attains the maximum upon the addition of 8 Λ's. Also in ^{378}120, a maximum binding energy is observed with the addition of 90 Λ's. In this way, we extract some lambda numbers, i.e., 2, 8, 18, 20, 40, 70, 90, which impart a maximum stability to the considered doubly magic nuclear cores and hence supposed to be Λ magic numbers as much as close to the numbers generated by the harmonic oscillator potential in the normal nuclear sector. But many of the strong signatures exist to identify the magicity and we make the analysis in this direction to look out for the correct Λ magic number. After analyzing the S_Λ and $S_{2\Lambda}$ for considered light to superheavy mass multi-hypernuclei, it is noticed that a sudden fall is observed at $\Lambda = 2, 8, 14, 20, 28, 34, 40, 50, 58, 68, 70$ and 82. And hence, the analysis suggest that these numbers are supposed to be Λ magic number in multi-Λ hypernuclei forming a triply magic system with doubly magic nucleonic core.

In order to identify the Λ magic number strongly, two-lambda shell gaps are examined which provide a stronger signature of magicity and also favour $S_{2\Lambda}$ results. Pronounced peak in two-lambda shell gap is observed at $\Lambda = 2, 8, 20$ and 40 indicating a strong shell closure. The peaks observed with a significant magnitude at Λ = 14, 18, 34, 50, 58, 70 and 82 indicating a shell closure also. Further to testify, we look for the lambda shell gaps by examining the single-particle energy levels. We noticed that a large single-particle gap appears in ^{208}Pb hypernucleus at $\Lambda = 2, 8, 18, 20, 28, 34, 40, 50, 58$ and 70 thus confirming these as the lambda magic numbers. The analysis of single-particle energy levels for ^{378}120 multi-hypernuclei supports the results manifested in large lambda shell gaps of 2, 8, 18, 20, 34, 40, 50, 58, 70 and 82. It is to be noted that a significant shell gap is also observed for 34 and 58, suggesting a strong Λ shell closure. The inversion of normal level scheme is responsible for the emergence the Λ magic numbers 34 and 58. The experimental confirmation of nucleonic shell closure of 34 supports our predictions.[85,86] The nucleonic number 14, 16, 18 and 32 have also been in discussion and expected to be shell closure.[87–90] In addition, nucleon numbers 16 and 32 have also been experimentally confirmed in exotic nuclei as a neutron magic number which is one of the predicted Λ shell closure in our calculations.[91,92] It is expected that the relatively weak strength of lambda spin-orbit interaction potential compared to nucleon-nucleon interaction is responsible for the emergence of the new lambda magic number other than the model scheme. The predicted Λ magic numbers in multi-hypernuclei are framed in Table 2. The present lambda magic numbers are in quite good agreement with the prediction of Refs. 13 and 79 where Bruckner–Hartee Fock calculations using the lambda density functional have been made. It is clear from the plot of $\delta_{2\Lambda}$ that 34, 58 and 70 have peaks of great magnitude, while 68 are in a feeble magnitude and supposed to be subshell closure. Moreover, strong nucleonic magic number 28 is observed to be very feeble in lambda magicity. It is of note that the lambda number 14 appears in medium mass hypernuclei and contrary to this 18 is observed in superheavy mass multi-hypernuclei. It is worth

Table 2. Lambda magic number produced in various considered multi-hypernuclei are tabulated here.

Hypernuclei	Lambda magic number												
$^{16+n\Lambda}$O	2	8	—	—	—	—	—	—	—	—	—	—	—
$^{48+n\Lambda}$Ca	2	8	14	—	20	—	—	—	—	—	—	—	—
$^{58+n\Lambda}$Ni	2	8	14	—	20	28	34	—	—	—	—	—	—
$^{90+n\Lambda}$Zr	2	8	14	—	20	28	—	40	50	—	—	—	—
$^{124+n\Lambda}$Sn	2	8	14	—	20	28	34	40	50	—	—	—	—
$^{132+n\Lambda}$Sn	2	8	14	—	20	28	34	40	50	—	—	—	—
$^{208+n\Lambda}$Pb	2	8	—	18	20	28	34	40	50	58	—	70	82
$^{292+n\Lambda}$120	2	8	—	18	—	28	34	40	50	58	68	—	82
$^{304+n\Lambda}$120	2	8	—	18	20	28	34	40	50	58	68	70	82
$^{378+n\Lambda}$120	2	8	14	18	20	—	34	40	50	58	68	—	82

mentioning that superheavy hypernuclei became strong candidates of new lambda shell closure of 34 and 58 other than the model scheme.

4. Summary and Conclusion

In summary, we have suggested the possible Λ magic number, i.e., 2, 8, 14, 18, 20, 28, 34, 40, 50, 58, 68, 70, 82 in multi-Λ hypernuclei within the RMF theory with effective ΛN as well as ΛΛ interactions. The survey of Λ magic number is made on the basis of binding energy, one- and two-lambda separation energies S_Λ, $S_{2\Lambda}$, and two-lambda shell gaps $\delta_{2\Lambda}$. It is noticed that pronounced single particle energy gap is observed for lambda number 34 and 58 in Pb and superheavy multi-hypernuclei representing the strong Λ magic number. Our results are kindly supported by nuclear magicity, where $N = 34$ is experimentally confirmed as a neutron magic number which is one of the Λ shell closure in our calculations.[85,86] It is expected that the relatively weak strength of lambda spin–orbit interaction potential compared to nucleon–nucleon interaction is responsible for the emergence of the new lambda magic number other than the model scheme. The predicted Λ magic numbers are in remarkable agreement with earlier predictions[13] and the predicted hypernuclear magicity quite resembles with nuclear magicity. It can therefore be concluded that YN interaction is same as NN ones with weaker strength. In analogy to the nuclear stability, we noticed a similar pattern of binding energy per particle in hypernuclear regime and Ni hypernucleus with 8 Λ's is found to be most tightly bound triply magic system in hypernuclear landscape. The addition of Λ hyperons has significant impact on nucleon distribution and removes the bubble structure partially or fully. The nucleon and lambda spin–orbit interaction potentials are also studied for the predicted triply magic hypernuclear systems and the added Λ's affect both the potentials to a large extent. The imparting of higher stability to the considered hypernuclear systems by the addition of certain number of lambdas in the present calculations may serve as a driving force for the production of triply magic hypernuclei experimentally in the near future. It is also concluded that the addition of Λ hyperons draws the nuclear system towards more stability

with increasing strangeness. We noticed that the core of superheavy nuclei has more affinity to absorb large number of hyperons. This means such systems are able to simulate the strange hadronic matter containing large number of heavy hyperons such as Σ's and Ξ's including several Λ's and the formation of such systems has large implication in nuclear-astrophysics.

Acknowledgments

One of the authors (MI) acknowledges the hospitality provided by Institute of Physics, Bhubaneswar during the work.

References

1. H. Bando, T. Motoba and J. Zofka, *Int. J. Mod. Phys. A* **5** (1990) 4021.
2. Y. Tan, X. Zhong, C. Cai and P. Ning, *Phys. Rev. C* **70** (2004) 054306.
3. B. Lu, E. Zhao and S. Zhou, *Phys. Rev. C* **84** (2011) 014328.
4. M. Rayet, *Ann. Phys.* **102** (1976) 226.
5. M. Rayet, *Nucl. Phys. A* **367** (1981) 381.
6. D. E. Lanskoy, *Phys. Rev. C* **58** (1998) 3351.
7. J. Meng *et al.*, *Prog. Part. Nucl. Phys.* **57** (2006) 470.
8. X.-R. Zhou, H.-J. Schulze, H. Sagawa, C.-X. Wu and E.-G. Zhao, *Phys. Rev. C* **76** (2007) 034312.
9. H. F. Lü, *Chin. Phys. Lett.* **25** (2008) 3613.
10. N. Guleria, S. K. Dhiman and R. Shyam, *Nucl. Phys. A* **886** (2012) 71.
11. F. Minto and K. Hagino, *Phys. Rev. C* **85** (2012) 024316.
12. A. Bouyssy, *Nucl. Phys. A* **381** (1982) 445.
13. J. Mares and J. Zofka, *Z. Phys. A* **333** (1989) 209.
14. M. Rufa, J. Schaffner, J. Maruhn H. Stöcker and W. Griner and P.-G. Reinhard, *Phys. Rev. C* **42** (1990) 2469.
15. J. Schaffner, C. Griner and H. St"ocker, *Phys. Rev. C* **46** (1992) 322.
16. J. Mares and J. Zofka, *Z. Phys. A* **345** (1993) 47.
17. J. Schaffner *et al.*, *Ann. Phys.* **235** (1994) 35.
18. E. N. E. Van Dalen, G. Colucci and A. D. Sedrakian, *Phys. Lett. B* **734** 383 (2014).
19. E. Hiyama, M. Kamimura, Y. Yamamoto, T. Motoba and T. A. Rijken, *Prog. Theor. Phys. Suppl.* **185** (2010) 106.
20. E. Hiyama, *Few-Body Syst.* **53** (2012) 189.
21. H. Nemura, S. Shinmura, Y. Akaishi and K. S. Myint, *Phys. Rev. Lett.* **94** (2005) 202502.
22. H. Nemura, S. Shinmura, Y. Akaishi and K. S. Myint, *Nucl. Phys. A* **754** (2005) 110c.
23. A. Gal, *Few-Body Syst.* **45** (2009) 105.
24. A. Gal and D. J. Millener, *Phys. Lett. B* **701** (2011) 342.
25. A. A. Usmani, *Phys. Rev. C* **73** (2006) 011302(R).
26. A. A. Usmani and F. C. Khanna, *J. Phys. G, Nucl. Part. Phys.* **35** (2008) 025105.
27. X.-R. Zhou, A. Polls, H.-J. Schulze and I. Vidaña, *Phys. Rev. C* **78** (2008) 054306.
28. I. Vidaña, A. Ramos and A. Polls, *Phys. Rev. C* **70** (2004) 024306.
29. C. Samanta, P. Roy Chowdhury and D. N. Basu, *J. Phys. G, Nucl. and Part. Phys.* **35** (2008) 065101.
30. D. E. Lenskoy and Y. Yamamoto, *Phys. Rev. C* **55** (1997) 2330.
31. J. Cugnon, A. Lejeune and H.-J. Schulze, *Phys. Rev. C* **62** (2000) 064308.

32. I. Vidana, A. Polls, A. Ramos and H.-J. Schulze, *Phys. Rev. C* **64** (2001) 044301.
33. M. Goeppert-Mayer and J. Jensen, *Elementary Theory of Nuclear Shell Structure* (Wiley, New York, 1955; Inostrannaya Literatura, Moscow, 1958).
34. V. G. Solovev, *Theory of Atomic Nuclei* (Energoizdat, Moscow, 1981; Institute of Physics, Bristol, England, 1992).
35. S. G. Nilsson and I. Ragnarsson, *Shapes and Shells in Nuclear Structure* (Cambridge University Press, Cambridge, England, 1995).
36. O. Sorlin and M.-G. Porquet, arXiv:0805.2561v1.
37. M. Bhuyan and S. K. Patra, *Mod. Phys. Lett. A* **27** (2012) 1250173.
38. W. Zhang, J. Meng, S. Q. Zhang, L. S. Geng and H. Toki, *Nucl. Phys. A* **753** (2005) 106.
39. V. M. Strutinsky, *Nucl. Phys. A* **95** (1967) 420.
40. V. M. Strutinsky, *Nucl. Phys. A* **122** (1998) 1.
41. S. K. Patra, R. K. Gupta and W. Greiner, *Mod. Phys. Lett. A* **12** (1997) 1727.
42. T. Sil, S. K. Patra, B. K. Sharma, M. Centelles and X. Vinas, *Phys. Rev. C* **69** (2004) 044315.
43. K. Rutz, M. Bender, T. Bürvenich, T. Schilling, P.-G. Reinhardt, J. A. Maruhn and W. Greiner, *Phys. Rev. C* **56** (1997) 238.
44. S. K. Patra, C.-L. Wu, C. R. Praharaj and R. K. Gupta, *Nucl. Phys. A* **651** (1999) 117.
45. J. Meng, H. Toki, S. Zhou, S. Zhang, W. Long and L. Geng, *Prog. Part. Nucl. Phys.* **57** (2007) 470.
46. S. K. Singh, M. Ikram and S. K. Patra, *Int. J. Mod. Phys. E* **22** (2013) 1350001.
47. B. D. Serot, *Rep. Prog. Phys.* **55** (1992) 1855.
48. Y. K. Gambhir, P. Ring and A. Thimet, *Ann. Phys.* (NY) **198** (1990) 132.
49. P. Ring, *Prog. Part. Nucl. Phys.* **37** (1996) 193.
50. B. D. Serot and J. D. Walecka, *Adv. Nucl. Phys. D* **16** (1986) 1.
51. J. Boguta and A. R. Bodmer, *Nucl. Phys. A* **292** (1977) 413.
52. T. K. Jha, P. K. Raina, P. K. Panda and S. K. Patra, *Phys. Rev. C* **74** (2007) 029903.
53. N. K. Glendenning and J. Schaffner, *Phys. Rev. Lett.* **81** (1998) 4564.
54. J. Schaffner, M. Hanauske, H. Stöcker and W. Greiner, *Phys. Rev. Lett.* **89** (2002) 171101.
55. Y. Sugahara and H. Toki, *Prog. Theor. Phys.* **92** (1994) 803.
56. D. Vretenar, W. Poschl, G. A. Lalazissis and P. Ring, *Phys. Rev. C* **57** (1998) R1060.
57. H.-F. Lü, J. Meng, S. Q. Zhang and S. G. Zhou, *Eur. Phys. J. A.* **17** (2003) 19.
58. H. Shen, F. Yang and H. Toki, *Prog. Theor. Phys.* **115** (2006) 325.
59. M. T. Win and K. Hagino, *Phys. Rev. C* **78** (2008) 054311.
60. M. Ikram, S. K. Singh, A. A. Usmani and S. K. Patra, *Int. J. Mod. Phys. E* **23** (2014) 1450052.
61. J. Schaffner, C. B. Dover, A. Gal, C. Greiner, D. J. Millener and H. Stöcker, *Ann. Phys.* (N.Y.) **235** (1994) 35.
62. J. Schaffner, C. B. Dover, A. Gal, C. Greiner and H. Stöcker, *Phys. Rev. Lett.* **71** (1993) 1328.
63. N. K. Glendenning, D. Von-Eiff, M. Haft, H. Lenske and M. K. Weigel, *Phys. Rev. C* **48** (1993) 889.
64. J. Mares and B. K. Jennings, *Phys. Rev. C* **49** (1994) 2472.
65. G. A. Lalazissis, S. Karatzikos, R. Fossion, D. Pena Arteaga, A. V. Afanasjev and P. Ring, *Phys. Lett. B* **671** (2009) 36.
66. C. B. Dover and A. Gal, *Prog. Part. Nucl. Phys.* **12** (1984) 171.

67. M. Chiapparini, M. E. Bracco, A. Delfino, M. Malheiro, D. P. Menezes and C. Providencia, *Nucl. Phys. A* **826** (2009) 178.
68. N. K. Glendenning and S. A. Moszkowski, *Phys. Rev. Lett.* **67** (1991) 2414.
69. O. Hashimoto and H. Tamura, *Prog. Part. Nucl. Phys.* **57** (2006) 564.
70. R. Xu, C. Wu and Z. Ren, *J. Phys. G., Nucl. Part. Phys.* **39** (2012) 085107.
71. E. Khan *et al.*, *Nucl. Phys. A* **800** (2008) 37.
72. J. Decharge *et al.*, *Nucl. Phys. A* **716** (2003) 55.
73. M. Grasso *et al.*, *Phys. Rev. C* **79** (2009) 034318.
74. Y. Z. Wang, J. Z. Gu, Z. Y. Li and Z. Y. Hou, *Eur. Phys. J. A* **15** (2013) 49.
75. H. Nakada, K. Sugimura and J. Margureon, *Phys. Rev. C* **87** (2013) 067305.
76. J. M. Yao, H. Mei and Z. P. Li, *Phys. Lett. B* **723** (2013) 459.
77. J. M. Yao, S. Baroni, M. Bender and P.-H. Heenen, *Phys. Rev. C* **86** (2012) 014310.
78. X. Y. Wu, T. M. Yao and Z. P. Li, *Phys. Rev. C* **89** (2014) 017304.
79. E. Khan, J. Margueron, F. Gulminelli and Ad. R. Raduta, *Phys. Rev. C* **92** (2015) 044313.
80. J. Boguta and S. Bohrmann, *Phys. Lett. B* **102** (1981) 93.
81. J. V. Noble, *Phys. Lett. B* **89** (1980) 325.
82. R. Brockmann and W. Weise, *Phys. Lett. B* **69** (1977) 167.
83. C. M. Keil, F. Hoffmann and H. Lenske, *Phys. Rev. C* **61** (2000) 064309.
84. S. Ajimura *et al.*, *Phys. Rev. Lett.* **86** (2001) 4255.
85. D. Steppenbeck *et al.*, *Nature* **502** (2013) 207.
86. P. Maierbeck *et al.*, *Phys. Lett. B* **675** (2009) 22.
87. T. R. Rodriguez and J. L. Egido, *Phys. Rev. Lett.* **99** (2007) 062501.
88. A. Ozawa *et al.*, *Phys. Rev. Lett.* **84** (2000) 5493.
89. R. Kanungo *et al.*, *Phys. Lett. B* **528** (2002) 58.
90. J. J. Li, J. Margueron, W. H. Long and N. V. Giai, *Phys. Lett. B* **753** (2016) 97.
91. R. Kanungo *et al.*, *Phys. Rev. Lett.* **102** (2009) 152501.
92. F. Wienholtz *et al.*, *Nature* **498** (2013) 346.